# Exploring the Concept of Dimerization-Induced Inter System Crossing: at the Origins of Spin-Orbit Coupling Selection Rules

Laura Abad Galán, José M Andrés Castán, Clément Dalinot, Pablo Simón Marqués, Joachim Galiana, Philippe Blanchard, Chantal Andraud, Elise Dumont, Olivier Maury, Clément Cabanetos, et al.

# Exploring the Concept of Dimerization-Induced Inter System Crossing: at the Origins of Spin-Orbit Coupling Selection Rules.

Laura Abad Galán,[a] José M. Andrés Castán,[b] Clément Dalinot,[b] Pablo Simón Marqués,[b] Joachim Galiana[a], Philippe Blanchard,[b] Chantal Andraud,[a] Elise Dumont[a,c], Olivier Maury,[a] Clément Cabanetos,[b]* Cyrille Monnereau,[a]* Tangui Le Bahers[a]*

[a] Univ Lyon, ENS de Lyon, CNRS UMR 5182, Université Claude Bernard Lyon 1, F-69342 Lyon, France.

[b] Univ Angers, CNRS UMR 6200, Moltech-Anjou, SFR-MATRIX, F-49045, Angers, France

[c] Institut Universitaire de France, 5 rue Descartes, Paris, 75005, France

**Abstract**

Singlet-Triplet interconversions and transitions (intersystem crossing, ISC) in organic molecules are at the basis of many important processes in cutting-edge photonic applications (Organic Light Emitting Devices, photodynamic therapy…). Selection rules for these transitions are mainly governed by the Spin-Orbit Coupling (SOC) phenomenon. Although the latter relies on complex relativistic phenomena, theoreticians have, with time, developed increasingly sophisticated and efficient approaches to gain access to a satisfactory evaluation of its magnitude. In this work, we bring a coupled experimental and theoretical analysis of the origin of the unusually large ISC efficiency on a series of dimers that differ by their nature (covalent or supramolecular) as well as the distance and relative orientation of their individual chromophoric components. The dynamical nature of the SOC, sometimes overlooked in literature, is discussed in deep.

The electronic structure of a standard organic molecule is generally formed by a singlet ground state ($S_0$), singlet excited states ($S_1$, $S_2$…) and triplet excited states ($T_1$, $T_2$…) which differ from the former by the alignment of the spins of their unpaired electrons.[1,2] The triplet states are generally lower in energy than the corresponding singlet states because of the stabilization exchange interaction between the electrons of same spins.[3] The control of the triplet states population and their energy is clearly a challenge because they are generally non-emissive ( "dark-states") as a result of restrictive selection rules in standard organic molecules, but are involved in multiple cutting-edge applications such as in molecular photonic, biology or photochemistry (e.g. OLEDs, photodynamic therapy, optical limiting…).[4–10] Nonetheless, a complete chemical and physical understanding and control of the properties of these states in elaborated organic molecules still lacks, and theoretical predictions often fail to provide a full picture of their energies, reactivities and evolutions. The forbidden character associated to a singlet-to-triplet state transition due to the spin selection rule using classical Hamiltonian can in certain instances be lifted thanks to the Spin-Orbit Coupling (SOC) through the Fermi's golden rule that can be written between $S_1$ and $T_1$ state (eq. 1-3 where $\rho(T_1)$ corresponds to the density of $T_1$ state at the $S_1$ energy, the summation of (2) is over electron indexes and the summation of (3) is over nucleus (see SI for all terms definition).[3,11]

$$\Gamma_{S_1 \to T_1} = \frac{2\pi}{\hbar} \left| \langle S_1 | \hat{H}_{SOC} | T_1 \rangle \right|^2 \rho(T_1) \tag{1}$$

$$\hat{H}_{SOC} = \sum_{i}^{n} A_i \left( \hat{l}_{x_i} \hat{s}_{x_i} + \hat{l}_{y_i} \hat{s}_{y_i} + \hat{l}_{z_i} \hat{s}_{z_i} \right) \tag{2}$$

$$A_i = \sum_{k}^{m} \frac{1}{r_{ik}^3} \frac{V(r_{ik})}{r_{ik}} \tag{3}$$

In this case, after initial excitation through light absorption or electro-stimulation, the interconversion between singlet and triplet excited states, called Inter-System Crossing (ISC), generally leads to the population of $T_1$, being the lowest excited state in energy.

The parameters that govern the SOC are clearly not straightforward. On organic molecules, the so-called El-Sayed rules predict that ISCs between states associated to $\pi \rightarrow \pi^*$ transitions are forbidden while $n \rightarrow \pi^*$ are authorized.[1] A generalization of these rules can be established by considerations of

group theory on the SOC Hamiltonian (eq (2)) as proposed by McClure in 1949.[11] Briefly, knowing that the angular momentum operator ($\hat{l}_{x,y,z_i}$) has the symmetry of the rotation operator, its product with $S_1$ and $T_1$ wavefunction representations must contain the totally symmetric representation to have a non-vanishing SOC. Overtime, several strategies were developed to overcome this selection rule.[12] Among those, it has been established that introducing a permanent distortion of the π-system of conjugated molecule (*i.e.* being a minimum on the potential energy surface, PES) or a dynamical one (*i.e.* temperature induced movement) can result in a large SOC between the $S_1$ and $T_1$ states.[2,6,13,14] A more recent approach consists in building dimers to mix the individual electronic states of monomers.[2,15–18] This process of *excitonic coupling* creates new triplet states of different symmetries below $S_1$ thus modifying the selection rules.

This can be illustrated with group theory considerations on the textbook case of *p*-cyanophenyl-ethynyl-aniline molecule (Figure 1).[19] The latter, in its monomeric form, is characterized by a $C_{2v}$ symmetry, a $^1A_1$ ground state, a $^1A_1$ lowest singlet excited state and a $^3A_1$ lowest triplet excited state. The $S_1$ ($^1A_1$) to $T_1$ ($^3A_1$) transition is both spin and symmetry forbidden, in compliance with El-Sayed's rule. Now, considering two limit cases of dimeric assemblies of this molecule (π-dimer or coplanar dimer, Figure 1) also belonging to the $C_{2v}$ group, it appears that in both cases, combination of $S_1$ and $T_1$ states of each individual subunit leads to a new $S_1$ state of $^1B_2$ representation and two triplet states below, of $^3B_2$ and $^3A_1$ representations. Interestingly, while the $S_1$ ($^1B_2$) to $T_1$ ($^3B_2$) transition remains both spin and symmetry forbidden, the $S_1$ to $T_2$ ($^3A_1$) transition now becomes symmetry allowed, causing partial relaxation of the El-Sayed rules. The symmetry allowed character of this new transition does not singlehandedly inform us about its expected intensity, which is only accessible by numerical calculation on the $S_1$-$T_n$ coupling through the SOC Hamiltonian (eq. (2)-(3)).

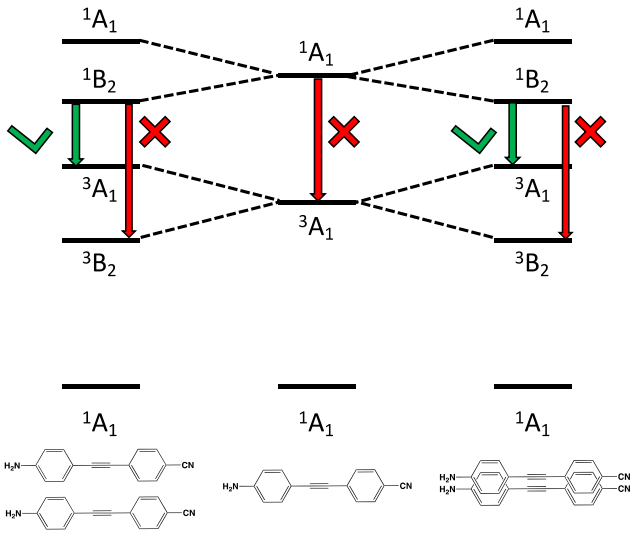


**Figure 1. Effect of dimerization on electronic states and the selection rules (symmetry only) of the $S_1$ to $T_n$ transitions of the *p*-cyanophenyl-ethynyl-aniline molecule (energy levels are arbitrary).**

In our ongoing efforts to expand this approach of tuning SOC intensity and ultimately ISC efficiency, we investigated the effects of excitonic coupling induced by dimerization on the SOC intensity of a series of benzothioxanthene imide derivatives **(**BTXI, **Figure 2**), which we recently identified as particularly relevant candidates for OLEDs applications.[20] Different chemical couplings were investigated, involving either direct C-C bond linkage between two **BTXI** units (***d*-BTXI**) or through a triazole-spacer (***t*-BTXI**). Finally, the effect of a through space, supramolecular $\pi$-dimer formation was investigated using the ***s*-BTXI** molecule, in which two BTXI units are connected to a central 1,4,7-triazacyclononane derivative.

In each case, the population of the triplet state was experimentally confirmed from low temperature phosphorescence measurements and indirectly quantified by evaluating the singlet oxygen generation efficiency of each system. Theoretically, the SOC intensity between $S_1$ and triplet states was computed at the TD-DFT level using a Douglas-Kroll Hamiltonian on $S_1$ optimized geometries, allowing systematic comparison between the experimental trends and theoretical predictions.[21]

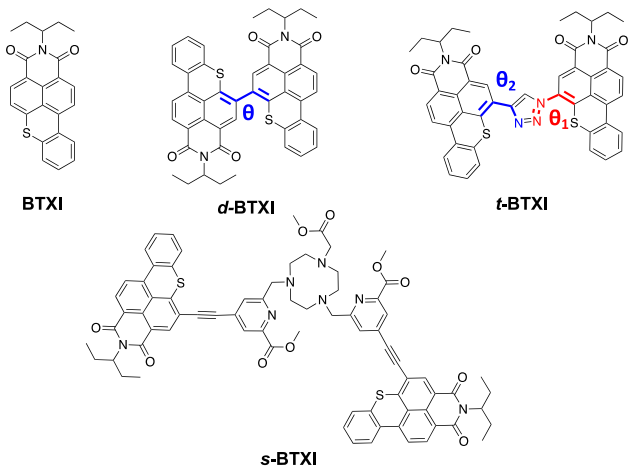


**Figure 2. Structures of the reference BTXI molecule and the herein investigated BTXI dimers.**

All the main photophysical data are summarized in **Table 1** while absorption and emission spectra and synthetic details are given in the **Supporting Information.** The features of the absorption and emission spectra for the three BTXI dimers very much resemble those of previously published BTXI molecules.[22] In our **BTXI** monomeric benchmark, luminescence quantum yield is close to unity. Consequently, no triplet signature can be found (phosphorescence signal at 77K or singlet oxygen generation). By comparison, dimerization of the molecule by direct C-C coupling (***d*-BTXI**) induces a clear enhancement of the ISC efficiency, as witnessed by a singlet oxygen generation efficiency that reaches 0.85, while fluorescence quantum yield is concomitantly reduced to 0.15. A clear signature of a long-lived phosphorescence signal at 77K is also detected using time-gated emission spectroscopy (**Figure S13**). Replacement of the direct C-C bond conjugation by a triazole π-linkage in the dimeric structure also impacts the ISC efficiency, although to a much lesser extent: singlet oxygen generation efficiency is therefore weaker, in comparison ($\mathbf{\Phi_\Delta}$ = 0.23), while fluorescence intensity remains high ($\mathbf{\Phi_f}$ = 0.56).

Interestingly, ***s*-BTXI** molecule, in which both BTXI subunits do not experience through-bond electronic communication is nevertheless characterized by a very strong ISC efficiency with $\mathbf{\Phi_\Delta}$ = 0.70 ($\mathbf{\Phi_f}$ = 0.28). Although devoid of direct electronic conjugation of the two subunits, through-space coupling of the transition dipole moments of each subunit (as a result of π-stacking, *vide infra*) appears strong enough to provide a large SOC between the newly generated mixed states.

These combined experimental data are a more sophisticated illustration of the simple concept presented in Figure 1: while for the monomer, the $\pi \rightarrow \pi^*$ character associated to the $S_1 \rightarrow T_1$ transition makes it strictly forbidden in compliance with El Sayed's rules, dimerization induced mixing of the excited states results in the occurrence of new symmetry allowed singlet-triplet transitions. However, this qualitative interpretation cannot bring a quantitative understanding of the different ISC efficiencies obtained from the different dimers and how those are related to the difference in the nature and magnitude of the excitonic coupling. Therefore, we took advantage of state-of-the-art quantum chemical calculations to bring quantitative insight into the origin of the enlargement in magnitude of the SOC.

| | $\lambda_{abs(max)}$ (nm) | $\lambda_{em}$ (nm) | $\Phi_f$ [a] | $\tau_{obs}$ (ns) | $k_r$ ($s^{-1}$) | $\Phi_\Delta$ [b] | $E_{Triplet}$ ($cm^{-1}$) |
|---|---|---|---|---|---|---|---|
| **BTXI** | 456 | 511 | 0.99 | 7.48 | $1.32 \times 10^8$ | 0.00 | - |
| ***d*-BTXI** | 455 | 509 | 0.15 | 2.15 | $8.84 \times 10^7$ | 0.85 | 15830 |
| ***t*-BTXI** | 458 | 520 | 0.56 | 6.91 | $8.10 \times 10^7$ | 0.23 | 15385 |
| **s-BTXI** | 466 | 514 | 0.28 | 7.41 | $7.41 \times 10^6$ | 0.70 | 14475 |

**Table 1. Highlighted photophysical properties of the studied molecules in diluted dichloromethane.**

Calculation of SOC between excited states is nowadays available using relatively widespread quantum chemical codes. Consequently, while a growing number of papers have used that powerful tool to analyse excited states properties, these calculations are mostly performed on a single optimized geometry of the molecule, that generally corresponds to the PES minimum at the $S_1$ state.[23–27] For flexible molecules, this approach may overlook or underestimate conformation effects at the origin of SOC enhancement. Some recent investigations have indeed highlighted the highly dynamical character of the SOC, which can be drastically affected by a molecular deformation (rotation, vibrational mode…).[8,13,28–32] In the specific case of dimeric molecules investigated herein, one can reasonably expect that the SOC strength could be affected by the nature of the coupling between the two monomers and particularly by the angle between their respective transition dipole moments. For the ***d*-BTXI** and ***t*-BTXI** dimers, the key geometrical parameters influencing this coupling are the dihedral angles between the two BTXI subunits ($\theta$ for ***d*-BTXI** and $\theta_1$ and $\theta_2$ for ***t*-BTXI**, **Figure 2**). In order to

investigate the influence of these parameters on SOC magnitude, relaxed scan at the $S_1$ state was performed to generate the $S_1$ PES as a function of these angles, at the TD-DFT cam-B3LYP level.[33] **Figure 3** and **S23-S24** present the $S_1$ PES and the SOC intensity as a function of the dihedral angles for ***d*-BTXI** and ***t*-BTXI**. While the most stable angle between the two monomers in ***d*-BTXI** is 30° as consequence of the steric repulsion, we can note that PES is very flat with a relatively small energy increase and thus the molecule explores the 30°-120° angle range at the $S_1$ state in standard temperature conditions. Similar conclusions can be drawn for ***t*-BTXI** with an even lower energy barrier for these rotations since the π-spacer minimizes steric repulsions between the BTXI subunits. We can consequently expect that the strength and nature of the excitonic coupling between the two monomers will strongly fluctuate according to their relative orientation.

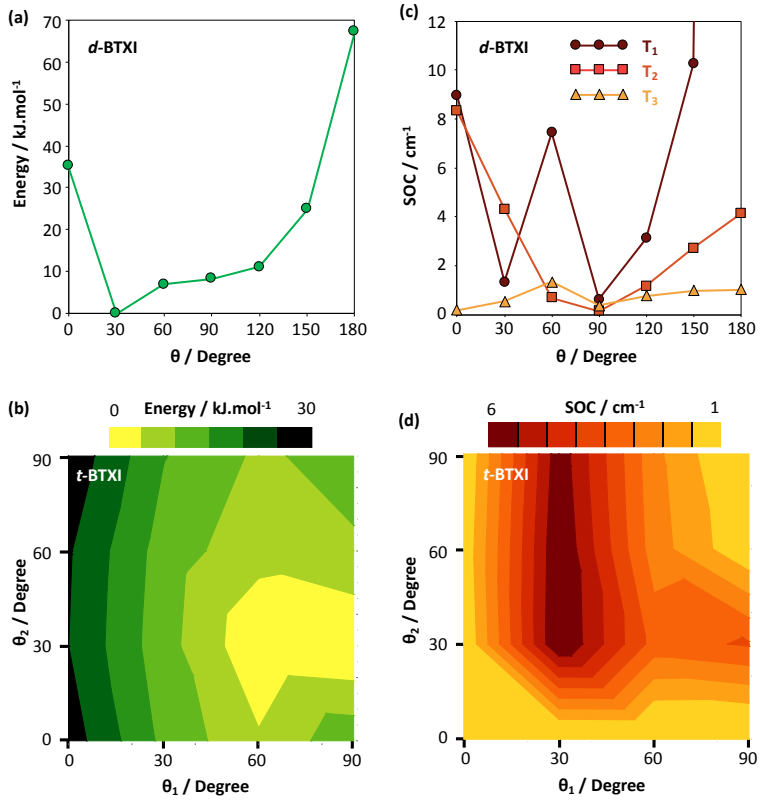


**Figure 3: Computed $S_1$ PES and SOC intensity as a function of the dihedral angles of the *d*-BTXI (a,c) and *t*-BTXI (b,d) molecules. For *t*-BTXI, only the $S_1$-$T_1$ coupling is presented, the coupling with $T_2$ and $T_3$ is given in SI.**

In contrast, **Figure 3** illustrates the extreme sensitivity of the SOC value (and thus of the expected ISC efficiencies) on the geometrical parameters. This information put in parallel with the relative flat PES supports the idea of the highly dynamic character of the SOC in these molecules. To gain a global

point of view, **Figure 4** summarizes the main results by presenting the energy range of the low-lying triplet states (using $S_1$ as a reference). Colours of the associated box plots represent the average value of the $S_1$-$T_n$ SOC. Compared to the **BTXI** monomer, we first find one additional triplet state below $S_1$ because of the mixing of the excited states as schematized on **Figure 1**. The energies of these triplet states are sensitive to the dihedral angles but to a higher extend for the directly connected dimer (***d*-BTXI**) compared to the ***t*-BTXI** in which the triazole π-linker weakens the interaction between the monomers. In compliance with our aforementioned considerations of the influence of excitonic coupling on ISC selection rules, the SOC in ***d*-BTXI** is much higher than that in **BTXI**. Finally, the SOC in ***d*-BTXI** is also notably higher than in ***t*-BTXI**, once again because the π-linker reduces the interaction between the two monomers.

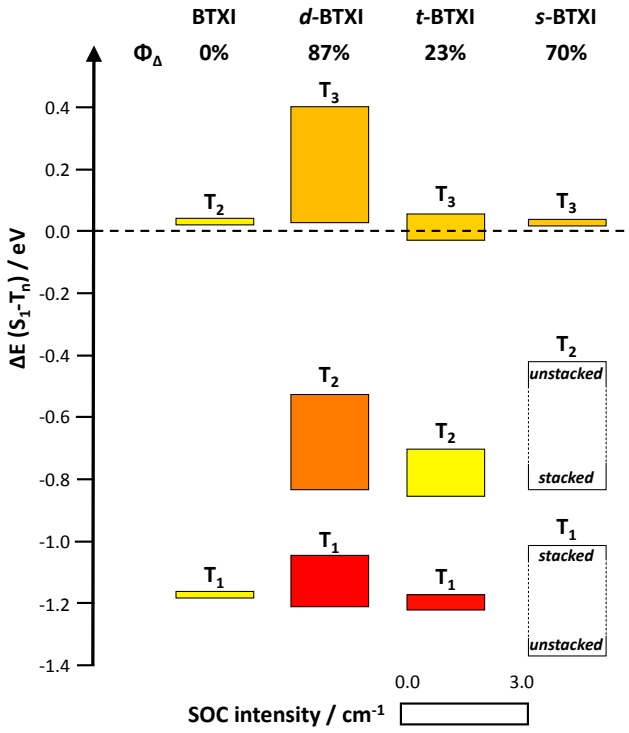


**Figure 4. Computed triplet states energy range, with $S_1$ as a reference energy, as a function of the molecular degrees of freedom considered in this work. Average SOC intensity is given in colour range and experimental singlet oxygen efficiency is given as well. Triplet energies and averaged SOCs are computed only on geometries not higher than 20 kJ.mol$^{-1}$ compared to the most stable geometry of the PES.**

Compared to the two other studied dimers, ***s*-BTXI** is conceptually different because there is no π-conjugation between the two monomers. Yet, the TACN-based linker connecting the two BTXI units offers enough flexibility to enable through-space formation of a supramolecular π-stacked dimeric arrangement of the two BTXI subunits. Classical molecular dynamics were performed on an open conformation of ***s*-BTXI** (see Figure S27), explicitly solvated in a $CH_2Cl_2$ cubic box, which corroborated a rapid dimerization. The latter is systematically observed in less than 10ns along ten independent trajectories, and the dimerization is maintained up to the microsecond range. After folding, the average distance between the two BTXI cores oscillates around 3.5±0.3 Å corroborating the formation of a stable π-dimer in good agreement with our hypothesis of a through space coupling of the BTXI subunits transition moment. The effect of this through space excitonic coupling on the SOC was investigated as for the two other dimers. However, ***s*-BTXI** considered as a supramolecular dimer with multiple degrees of freedom, the definition of a single geometrical descriptor governing the strength of the electronic coupling between the two units is less obvious. In the latter case, only two geometries of ***s*-BTXI** were considered and both optimized at the $S_1$ state (**Figure S25**). Hence, while the two BTXI subunits are π-stacked in the first one (3.4 Å between the two BTXI units), the two BTXI units are far from each other in the second (13.7 Å between the two BTXI units). The positions of triplet states and SOC intensities computed for these two geometries are considered to give the extremum of fluctuation of these properties for this molecule (**Figure 4**). As for the two other dimers, the interaction between the two BTXIs in ***s*-BTXI** leads to two triplet states below $S_1$ having large energy fluctuations and even as large as for the ***d*-BTXI** molecule. A noteworthy increase of the SOC is computed (0.5 $cm^{-1}$ for the π-stacked structure) compared to BTXI monomer (0.1 $cm^{-1}$) due to the through space excitonic coupling between the two units as illustrated by the $S_1$-$T_n$ variation of electron density (**Figure S26**), even though the intensity of the SOC is not as strong as for the other two π-conjugated dimers.

Thus, in spite of the qualitative agreement between our calculations and the observed experimental trend, considerations based exclusively on calculated SOC partly fail to quantitatively explain the efficiency of the ISC process in ***s*-BTXI**. In order to fully address this issue, another important

parameter which has been omitted to the discussion up to now must be considered. For ***d*-BTXI** and ***t*-BTXI**, the dynamical relative oblique arrangement of BTXI subunits leads to a non-parallel orientation of the transition dipole resulting in what is sometimes called a J/H excitonic coupling in solids:[34] although both calculated oscillator strength and measured $k_r$ appear slightly decreased compared to our BTXI benchmark, in agreement with theory, their value remains high (**Table 1**). In contrast, in ***s*-BTXI,** the two BTXI subunits stack on top of each other, giving rise in this case (still by analogy with solids) to an H-type excitonic interaction.[16] A well-established consequence of that type of organisation is that the radiative transition from the lowest singlet excited state ($S_1$) to the ground state takes a partly forbidden character. This character is both illustrated by calculations, which predict an oscillator strength in emission (f = 0.2) about three times lower than that of the **BTXI** (f = 0.6) and by experimental measurements with a calculated $k_r$ one order of magnitude lower for ***s*-BTXI** than for the other **BTXI** and ***d*-BTXI** molecules (**Table 1**). As a consequence, for ***s*-*d*-BTXI**, the relatively weak SOC in comparison with other dimers is compensated by a lower radiative decay kinetics (see Supporting Information).

To conclude on these investigations, the dimerization strategy appears to be a particularly effective way to overcome El-Sayed rules. In the case of this particular study, mixing of the individual electronic states of each BTXI subunit ultimately leads to strongly allowed $S_1$-$T_n$ transitions. Interestingly, we found that the dimerization induced SOC enhancement can be obtained not only by direct covalent coupling between both subunits, but more interestingly in the framework of supramolecular assemblies. The relative orientations between each subunit strongly affects both the triplet energies and the SOC intensity. The last point is particularly appealing, since considering the SOC as a dynamical phenomenon sensitive to molecular distortion may inspire new strategies towards a chemical engineering of actuators based on singlet-triplet equilibria, which could represent a relevant step in the development of future photonics devices.

**Acknowledgement**

LAG thanks Agence Nationale de la Recherche (SADAM ANR-16-CE07-0015-02) for her grant. TLB and ED are grateful to the SYSPROD project and AXELERA Pôle de Compétitivité for financial support (PSMN Data Center). J. M. A. C. and P. S. M. acknowledge the European Union's Horizon 2020 research and innovation program under Marie Sklodowska Curie Grant agreement No. 722651 (SEPOMO). The Région Pays de la Loire is also acknowledged for the Projet « étoiles montantes SAMOA».

**Supporting Information**

Supporting Information provides all experimental and computational details, all absorption and emission spectra measured at room temperature and 77K, computed $S_1$-$T_n$ energy gap of ***d*-BTXI** and ***t*-BTXI**, computed $S_1$-$T_n$ SOC of ***t*-BTXI**, computed variation of electron density between $S_1$ and $T_n$ of ***s*-BTXI** and most stable optimized structures in cartesian coordinate.

**References:**


(1) Lower, S. K.; El-Sayed, M. A. The Triplet State and Molecular Electronic Processes in Organic Molecules. *Chem. Rev.* **1966**, *66* (2), 199–241.

(2) Sasikumar, D.; John, A. T.; Sunny, J.; Hariharan, M. Access to the Triplet Excited States of Organic Chromophores. *Chem. Soc. Rev.* **2020**, *49* (17), 6122–6140.

(3) Baryshnikov, G.; Minaev, B.; Ågren, H. Theory and Calculation of the Phosphorescence Phenomenon. *Chem. Rev.* **2017**, *117* (9), 6500–6537.

(4) Zhao, J.; Wu, W.; Sun, J.; Guo, S. Triplet Photosensitizers: From Molecular Design to Applications. *Chem. Soc. Rev.* **2013**, *42* (12), 5323–5351.

(5) Miyata, K.; Conrad-Burton, F. S.; Geyer, F. L.; Zhu, X. Y. Triplet Pair States in Singlet Fission. *Chem. Rev.* **2019**, *119* (6), 4261–4292.

(6) Chen, X. K.; Kim, D.; Brédas, J. L. Thermally Activated Delayed Fluorescence (TADF) Path toward Efficient Electroluminescence in Purely Organic Materials: Molecular Level Insight. *Acc. Chem. Res.* **2018**, *51* (9), 2215–2224.

(7) Wex, B.; Kaafarani, B. R. Perspective on Carbazole-Based Organic Compounds as Emitters and Hosts in TADF Applications. *J. Mater. Chem. C* **2017**, *5* (34), 8622–8653.

(8) Hu, W.; Prasad, P. N.; Huang, W. Manipulating the Dynamics of Dark Excited States in Organic Materials for Phototheranostics. *Acc. Chem. Res.* **2021**, *54*, 697–706.

(9) Lundén, H.; Pitrat, D.; Mulatier, J. C.; Monnereau, C.; Minda, I.; Liotta, A.; Chábera, P.; Hopen, D. K.; Lopes, C.; Parola, S.; et al. An Optical Power Limiting and Ultrafast Photophysics Investigation of a Series of Multi-Branched Heavy Atom Substituted Fluorene Molecules. *Inorganics* **2019**, *7* (10), 1–15.

(10) Chateau, D.; Chaput, F.; Lopes, C.; Lindgren, M.; Brännlund, C.; Öhgren, J.; Djourelov, N.; Nedelec, P.; Desroches, C.; Eliasson, B.; et al. Silica Hybrid Sol-Gel Materials with Unusually High Concentration of Ptorganic Molecular Guests: Studies of Luminescence and Nonlinear

Absorption of Light. *ACS Appl. Mater. Inter.* **2012**, *4* (5), 2369–2377.

(11) McClure, D. S. Selection Rules for Singlet-Triplet Perturbations in Polyatomic Molecules. *J. Chem. Phys.* **1949**, *17* (7), 665–666.

(12) Nguyen, V. N.; Yan, Y.; Zhao, J.; Yoon, J. Heavy-Atom-Free Photosensitizers: From Molecular Design to Applications in the Photodynamic Therapy of Cancer. *Acc. Chem. Res* **2021**, *54* (1), 207–220.

(13) Penfold, T. J.; Gindensperger, E.; Daniel, C.; Marian, C. M. Spin-Vibronic Mechanism for Intersystem Crossing. *Chem. Rev.* **2018**, *118* (15), 6975–7025.

(14) Demangeat, A. C.; Dou, Y.; Hu, B.; Bretonnière, Y.; Andraud, C.; D'Aléo, A.; Wu, J. W.; Kim, E.; Le Bahers, T.; Attias, A.-J. σ-Conjugation and H-Bond-Directed Supramolecular Self-Assembly: Key Features for Efficient Long-Lived Room Temperature Phosphorescent Organic Molecular Crystals Catherine. *Angew. Chem. Int. Ed.* **2020**, *133*, 2476–2484.

(15) Dos Santos, P. L.; Dias, F. B.; Monkman, A. P. Investigation of the Mechanisms Giving Rise to TADF in Exciplex States. *J. Phys. Chem. C* **2016**, *120* (32), 18259–18267.

(16) An, Z.; Zheng, C.; Tao, Y.; Chen, R.; Shi, H.; Chen, T.; Wang, Z.; Li, H.; Deng, R.; Liu, X.; et al. Stabilizing Triplet Excited States for Ultralong Organic Phosphorescence. *Nat. Mater.* **2015**, *14* (7), 685–690.

(17) Darghouth, A. A. M. H. M.; Correa, G. C.; Juillard, S.; Casida, M. E.; Humeniuk, A.; Mitrić, R. Davydov-Type Excitonic Effects on the Absorption Spectra of Parallel-Stacked and Herringbone Aggregates of Pentacene: Time-Dependent Density-Functional Theory and Time-Dependent Density-Functional Tight Binding. *J. Chem. Phys.* **2018**, *149*, 134111.

(18) Pabst, M.; Lunkenheimer, B.; Köhn, A. The Triplet Excimer of Naphthalene: A Model System for Triplet-Triplet Interactions and Its Spectral Properties. *J. Phys. Chem. C* **2011**, *115* (16), 8335–8344.

(19) Marek, Z.; Edward, C.; Fujiwara, T.; Zgierski, M. Z.; Lim, E. C. NRC Publications Archive

Archives Des Publications Du CNRC Combined Experimental and Computational Study of Intramolecular Combined Experimental and Computational Study of Intramolecular Charge Transfer In p - N , N -Dimethylamino- p 0 -Cyano-Diphenylacet. *J. Phys. Chem. A* **2011**, *115*, 586–592.

(20) Galán, L. A.; Andrés Castán, J. M.; Dalinot, C.; Marqués, P. S.; Blanchard, P.; Maury, O.; Cabanetos, C.; Le Bahers, T.; Monnereau, C. Theoretical and Experimental Investigation on the Intersystem Crossing Kinetics in Benzothioxanthene Imide Luminophores, and Their Dependence on Substituent Effects. *Phys. Chem. Chem. Phys.* **2020**, *22*, 12373–12381.

(21) Nakajima, T.; Transformation, D. À. K.; Kroll, H. A. D. À. The Douglas À Kroll À Hess Approach. *Chem. Rev.* **2012**, *112*, 385–402.

(22) Andrés Castán, J. M.; Abad Galán, L.; Li, S.; Dalinot, C.; Simón Marqués, P.; Allain, M.; Risko, C.; Monnereau, C.; Maury, O.; Blanchard, P.; et al. Nitration of Benzothioxanthene: Towards a New Class of Dyes with Versatile Photophysical Properties. *New J. Chem.* **2020**, *44* (3), 900–905.

(23) Yang, W.; Zhao, J.; Sonn, C.; Escudero, D.; Karatay, A.; Yaglioglu, H. G.; Küçükoz, B.; Hayvali, M.; Li, C.; Jacquemin, D. Efficient Intersystem Crossing in Heavy-Atom-Free Perylenebisimide Derivatives. *J. Phys. Chem. C* **2016**, *120* (19), 10162–10175.

(24) Wang, X.; Yin, X.; Lai, X. Y.; Liu, Y. T. A Theoretical Study of a Series of Water-Soluble Triphenylamine Photosensitizers for Two-Photon Photodynamic Therapy. *Spectrochim. Acta. A* **2018**, *203*, 229–235.

(25) Hou, Y.; Biskup, T.; Rein, S.; Wang, Z.; Bussotti, L.; Russo, N.; Foggi, P.; Zhao, J.; Di Donato, M.; Mazzone, G.; et al. Spin-Orbit Charge Recombination Intersystem Crossing in Phenothiazine-Anthracene Compact Dyads: Effect of Molecular Conformation on Electronic Coupling, Electronic Transitions, and Electron Spin Polarizations of the Triplet States. *J. Phys. Chem. C* **2018**, *122* (49), 27850–27865.

(26) Alberto, M. E.; Mazzone, G.; Quartarolo, A. D.; Sousa, F. F. R.; Sicilia, E.; Russo, N. Electronic Spectra and Intersystem Spin-Orbit Coupling in 1,2- and 1,3-Squaraines. *J. Comput. Chem.* **2014**, *35* (29), 2107–2113.

(27) Gao, X.; Bai, S.; Fazzi, D.; Niehaus, T.; Barbatti, M.; Thiel, W. Evaluation of Spin-Orbit Couplings with Linear-Response Time-Dependent Density Functional Methods. *J. Chem. Theory Comput.* **2017**, *13* (2), 515–524.

(28) Higginbotham, H. F.; Yi, C. L.; Monkman, A. P.; Wong, K. T. Effects of Ortho-Phenyl Substitution on the RISC Rate of D-A Type TADF Molecules. *J. Phys. Chem. C* **2018**, *122* (14), 7627–7634.

(29) Gibson, J.; Monkman, A. P.; Penfold, T. J. The Importance of Vibronic Coupling for Efficient Reverse Intersystem Crossing in Thermally Activated Delayed Fluorescence Molecules. *ChemPhysChem* **2016**, No. 1, 2956–2961.

(30) Kim, D. H.; D'Aléo, A.; Chen, X. K.; Sandanayaka, A. D. S.; Yao, D.; Zhao, L.; Komino, T.; Zaborova, E.; Canard, G.; Tsuchiya, Y.; et al. High-Efficiency Electroluminescence and Amplified Spontaneous Emission from a Thermally Activated Delayed Fluorescent near-Infrared Emitter. *Nat. Photonics* **2018**, *12* (2), 98–104.

(31) Galland, M.; Le Bahers, T.; Banyasz, A.; Lascoux, N.; Duperray, A.; Grichine, A.; Tripier, R.; Guyot, Y.; Maynadier, M.; Nguyen, C.; et al. A "Multi-Heavy-Atom" Approach toward Biphotonic Photosensitizers with Improved Singlet-Oxygen Generation Properties. *Chem. Eur. J.* **2019**, *25* (38), 9026–9034.

(32) Mettra, B.; Liao, Y. Y.; Gallavardin, T.; Armagnat, C.; Pitrat, D.; Baldeck, P.; Le Bahers, T.; Monnereau, C.; Andraud, C. A Combined Theoretical and Experimental Investigation on the Influence of the Bromine Substitution Pattern on the Photophysics of Conjugated Organic Chromophores. *Phys. Chem. Chem. Phys.* **2018**, *20* (5), 3768–3783.

(33) Yanai, T.; Tew, D. P.; Handy, N. C. A New Hybrid Exchange–Correlation Functional Using

the Coulomb-Attenuating Method (CAM-B3LYP). *Chem. Phys. Lett.* **2004**, *393*, 51–57.

(34) Fothergill, J. W.; Hernandez, A. C.; Knowlton, W. B.; Yurke, B.; Li, L. Ab Initio Studies of Exciton Interactions of Cy5 Dyes. *J. Phys. Chem. A.* **2018**, *122* (46), 8989–8997.

**Table of Content**